Applied Physics B (2020) 126:106
https://doi.org/10.1007/s00340-020-07464-x

**Applied Physics B**
**Lasers and Optics**


# Long-term stable 850-Hz linewidth single-longitudinal-mode ring cavity fiber laser using polarization-maintaining fiber

**Haowei Liu[1,2] · Qiao Lu[1] · Shanshan Wei[1,3] · Bo Yao[1] · Li Wei[4] · Qinghe Mao[1,3]**

Received: 2 November 2019 / Accepted: 13 May 2020 / Published online: 21 May 2020


**Abstract**
A long-term stable single-longitudinal-mode (SLM) all polarization-maintaining (PM) compound-ring cavity fiber laser is reported. The results show that the PM fiber's strong ability to resist the environment disturbance allows finely designing the length of each secondary cavity in real time according to the main cavity under the laboratory environment, and then the effective longitudinal mode spacing can be sufficiently increased by accurately using the Vernier effect, so that the mode-hopping can be effectively suppressed. Furthermore, the temperature compensation is used for asynchronously fine-adjusting each cavity length to follow the Vernier effect requirement more strictly. The mode-hopping-free SLM operation time of the packaged laser reaches 11 h. As far as we know, this is the longest SLM free running time of ring cavity fiber laser to date. The optical signal to noise ratio of the laser reaches 77 dB and the linewidth is less than 850 Hz with up to 50 mW maximum output power.

## 1 Introduction

Low noise narrow-linewidth single-longitudinal-mode (SLM) lasers have very important applications in many fields, such as gravitational wave detection [1], atomic and molecular physics [2], precision measurement [3] and generating the cylindrical vector beams (CVBs) [4, 5]. Over the past decades, the stability of SLM fiber laser has improved greatly [6], its noise has been effectively suppressed [7], and linewidth continues to be narrowed [8]. Therefore, combined with its intrinsic flexibility and good beam quality, the SLM fiber laser has become an extremely important seed laser source in various applications. Currently, the cavities of SLM fiber laser may be generally divided into three schemes: distributed feedback [9], distributed Bragg reflection [10], and ring cavity [11]. Among them, the ring cavity permits using a long cavity design, which is helpful to offer different operation functions, such as frequency tuning and feedback control, by simply inserting optical components into the cavity [6, 12]. This also facilitates an increase in the cavity gain with relatively long gain fibers to improve output power and narrow linewidth [13]. However, as the free spectral range (FSR) for a ring cavity with length beyond 1 m is less than 200 MHz, more than $10^4$–$10^5$ potential longitudinal modes may exist within the gain bandwidth of the doped fiber. Meanwhile, the homogeneous gain broadening of the gain fiber is always accompanied by some inhomogeneous broadening [14, 15]. Thus, multi-longitudinal mode oscillation or mode-hopping may be unavoidable for the ring cavity laser. For this reason, different compound cavity configurations have been proposed to suppress the mode-hopping using the Vernier effect to increase the effective longitudinal mode spacing [12, 16–19], including supplementation by the narrow band filtering [16–18] and the saturable absorption effect of the gain fiber [12, 19, 20].

The mode-hopping of the fiber laser mainly originates from the external environmental disturbance to the cavity length in particular, the long cavity length of the ring cavity. Therefore, several techniques, including vibration isolation [17], thermal insulation [20], and active feedback scheme based on phase-sensitive detection [6, 21], have been used to prolong the mode-hopping-free SLM operation time of the

✉ Qinghe Mao
mqinghe@aiofm.ac.cn

[1] Anhui Provincial Key Laboratory of Photonics Devices and Materials, Anhui Institute of Optics and Fine Mechanics, Chinese Academy of Sciences, Hefei 230031, Anhui, China

[2] University of Chinese Academy of Sciences, Beijing 100049, China

[3] University of Science and Technology of China, Hefei 230026, Anhui, China

[4] Department of Physics and Computer Science, Wilfrid Laurier University, Waterloo, ON N2L 3C5, Canada

ring cavity fiber laser. Yet, it remains difficult to meet the needs of practical applications. However, polarization maintaining (PM) fibers have been extensively used in passive mode-locked fiber lasers and optical frequency combs [22]. The results show that PM fiber can significantly improve the ability of fiber lasers to resist environmental disturbances. In the so-called "δ" type SLM fiber lasers, the use of PM fibers has also been seen to suppress environmental noise [21]. However, thus far, there has been no research on the design of all-PM compound ring cavity fiber laser which is, in principle, more likely to achieve long-term SLM operation. If all the fiber used in a compound ring cavity fiber laser is PM fiber, the strong ability of the latter to resist external disturbance may be used to design the length of each secondary cavity accurately and in real time. This would substantially increase the effective longitudinal mode spacing through the strict Vernier effect, which would in turn greatly improve the stability of the SLM operation and thus fundamentally eliminate the occurrence of mode-hopping. However, to the best of our knowledge, no relevant research on this has been reported as yet.

This paper describes a narrow-linewidth SLM compound ring cavity erbium-doped fiber (EDF) laser based on PM fiber. The PM fiber has a strong ability to resist external disturbances; thus, the length of the secondary cavities can be optimized in real time, according to the main cavity length, to widen the effective longitudinal mode spacing of the composite cavity as the requirements of the Vernier effect. This can effectively suppress the mode-hopping of the laser in a laboratory environment. The cavity length can be further controlled by temperature compensation so that it can meet the requirements of the Vernier effect precisely, thereby suppressing the mode-hopping of the packaged laser and improving the long-term stability of SLM operation.

## 2 Experimental setup

Figure 1 illustrates the schematic of our SLM compound ring cavity EDF laser with the PM fiber. A segment of 0.66 m-long PM EDF (PM-ESF-7/125, Nufern) with an absorption of 20 dB/m at 975 nm was used as the gain fiber, which was pumped by a 975 nm diode laser with 600 mW maximum output power through a PM wavelength division multiplexer (PM-WDM). A fast-axis-blocked PM circulator (PM-CIR) was inserted into the main cavity. A 1560.4 nm PM fiber Bragg grating (PM-FBG) with 99% reflectivity and 0.1 nm 3-dB bandwidth (corresponding to 12.3 GHz) was connected to the common port of the PM-CIR to form a narrow-band filter in the main cavity, to reduce the potential longitudinal modes in the gain bandwidth. Moreover, the unidirectional propagation of the light wave and suppression of coupling between two orthogonal polarization states

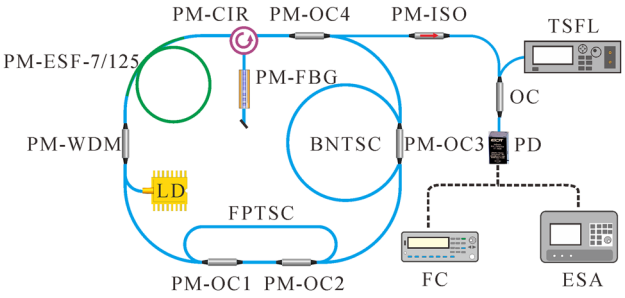


**Fig. 1** Schematic of the all-PM SLM compound ring cavity fiber laser and the automatic mode-hopping monitoring system. *PM* polarization-maintaining, *FBG* fiber Bragg grating, *OC* optical coupler, *WDM* wavelength division multiplexer, *ISO* fiber isolator, *PD* photodetector, *TSFL* tunable single frequency laser, *FC* frequency counter, *ESA* electric spectrum analyser, *LD* laser diode, *FPTSC* F-P type secondary cavity, *BNTSC* band-notch type secondary cavity

could be achieved in the cavity by the PM-CIR. A pair of PM fiber couplers (PM-OC1 and PM-OC2) was used to form an F-P type ring resonator. This F-P type cavity was inserted into the main cavity as a secondary cavity; the very narrow resonant transmission peaks of the F-P type cavity were used to filter out a potentially oscillating longitudinal mode from a large number of main cavity longitudinal modes with very small mode spacing [17]. A band-notch type resonator, constructed with a 50:50 PM-OC3, was also inserted into the main cavity as another secondary cavity. The stop band of this secondary cavity was used to suppress the excess dominant main cavity modes in the FBG bandwidth selected by the F-P type secondary cavity. All the open pigtail fibers were cleaved at 8° to suppress the reflections of the fiber end facets. A PM fiber coupler with a 50:50 coupling ratio, PM-OC4, was used to couple the laser out, and a PM isolator (PM-ISO) was spliced to the output port to prevent external reflection. To suppress mode-hopping and improve stability, the length of the main cavity was designed to be as short as possible. Considering that the bandwidth and transmittance of the F-P type secondary cavity's resonant peaks were related to the coupling ratio of the used PM-OCs [23], a 70:30 coupling ratio for PM-OC1 and PM-OC2 was implemented based on the actual length of the main cavity; this ensured that only one main cavity longitudinal mode could be located in the 3 dB bandwidth of the F-P type cavity's resonant transmission peak, while the insert loss of the secondary cavity could be as low as possible. The length of the F-P type secondary cavity was also designed to be as short as possible, while the length of the band-notch type secondary cavity was required to be designed according to both the lengths of the main cavity and the F-P type secondary cavity (the details are shown in Sect. 3).

Because the FBG reflection characteristic is extremely sensitive to environmental disturbances, it impedes the optimization of the lengths of the two secondary cavities in a

laboratory environment. Therefore, in this study, the FBG was independently packaged using the temperature-compensated technique. After packaging, the central wavelength of the FBG varied with temperature below 1 pm/℃ (corresponding to ~ 120 MHz/℃). When the laser was optimized, it was packaged into a double-decked box constructed with the polytetrafluoroethylene (PTFE) outside and aluminum plate inside to suppress the influence of environmental vibration and thermal disturbance. A precision temperature control with controlling accuracy of 0.1 ℃ was also equipped with the box. The output SLM laser was measured by an optical power meter (Ophir, Vega7ZO1560), an optical spectrum analyser (Yokogawa, AQ6370D), an F-P scanning interferometer (Thorlabs, SA200-12B or SA210-12B), a photodetector (EOT, ET3000A) followed by an electric spectrum analyser (ESA, Agilent, E4402B) and a delayed self-heterodyne system. A commercial tunable single frequency laser (TSFL, Agilent, 8164B) was used to beat with our laser in the photodetector. The beat signal was recorded automatically by a frequency counter (Agilent, 53220A) to study the mode-hopping and frequency-drift characteristics of our SLM laser.

## 3 Results and discussions

Our experiment first studied the SLM oscillation behavior of the laser when only the F-P type secondary cavity was inserted into the main cavity. The main cavity length was 1.66 m, and the corresponding FSR was ~ 125 MHz. When the 0.51 m long F-P type secondary cavity was inserted (the corresponding FSR was ~ 406 MHz), two types of F-P scanning interferometers, with scanning ranges of 1.5 GHz and 10 GHz, respectively, were used to monitor the longitudinal mode oscillations. The purpose of using the scanning ranges of 1.5 GHz and 10 GHz here is to catch the possible mode-hopping that may be closer and far away from the oscillating longitudinal mode. The results show that the laser may operate in the SLM state, which is a reasonable result of expanding the effective longitudinal mode spacing by the Vernier effect between the main cavity and the F-P type secondary cavity; however, the SLM lasing can only last for a few minutes. This may be due to the fact that the oscillating main cavity longitudinal mode selected by a certain resonant transmission peak of the F-P cavity may not be right in the center of the resonant transmission peak, allowing the other resonant transmission peaks of the F-P type cavity to pick out other main cavity modes that are able to compete with the oscillating main cavity mode. For this reason, the length of the F-P type secondary cavity was carefully changed in 1 mm steps while the main cavity length was kept unchanged. It was found that the SLM continuous operation time varied almost periodically with the increase or decrease of the length of the F-P type cavity, which may be caused by the vernier effect in the process of increasing or decreasing the length of the F-P type secondary cavity only. When the length of the F-P cavity was 0.5 m and the corresponding FSR was 414 MHz, the SLM operation time of the laser without mode-hopping could reach 7 min. Figure 2a shows the SLM oscillation of the laser monitored by the F-P scanning interferometer. This indicates that by optimizing the length of the F-P secondary cavity, the oscillating main cavity mode selected by the resonant transmission peak can be adjusted closer to the center of the resonant transmission peak, resulting in a more dominant position of the oscillating mode when competing with other main cavity modes. It is worth noting that the ability to continuously optimize the length of the F-P secondary cavity in real time to select a more dominant oscillating main cavity mode by monitoring the F-P scanning interferometer in the laboratory environment depends on using PM fiber with strong resistance to external disturbance, which is difficult to achieve in a non-PM compound ring cavity fiber laser [17].

However, if only the F-P type secondary cavity is inserted into the main cavity, mode-hopping will occur in the laser even if the length of the F-P type secondary cavity has been fine optimized as per the main cavity length. Moreover, the mode-hopping observed by the F-P scanning interferometer generally occurs in the same position. Figure 2b shows the mode-hopping phenomenon captured by the F-P scanning interferometer. This, combined with monitoring via the ESA, showed that the mode-hopping occurred at a lower frequency position. There was a difference of ~ 1.2 GHz from the dominant oscillating longitudinal mode, indicating that there was a redundant dominant main cavity mode selected by the F-P type secondary cavity in the bandwidth of the FBG filter (see Fig. 2c). Thus, we inserted the band-notch cavity into the main cavity, using its stop band to suppress the possible mode competition from the redundant dominant main cavity mode. As the length of the main cavity would increase when the band-notch type secondary cavity was inserted into the main cavity, the lengths of the main cavity and the F-P type secondary cavity required re-optimization by the aforementioned method. After optimization, their cavity lengths and the corresponding FSRs were changed to 2.26 and 0.49 m, and 92 and 422 MHz, respectively. On this basis, that is, keeping the length of the main cavity and the F-P type secondary cavity unchanged at 2.26 m and 0.49 m, respectively, the cavity length of the band-notch secondary cavity was carefully optimized by monitoring the F-P scanning interferometer. When the length of the band-notch secondary cavity was 1.86 m, the stable SLM operation time of the laser increased to 15–20 min. Figure 2d shows the characteristics of SLM oscillation as monitored by the F-P interferometer. The result indicates that the band-notch secondary cavity suppressed the some potential sub-dominant

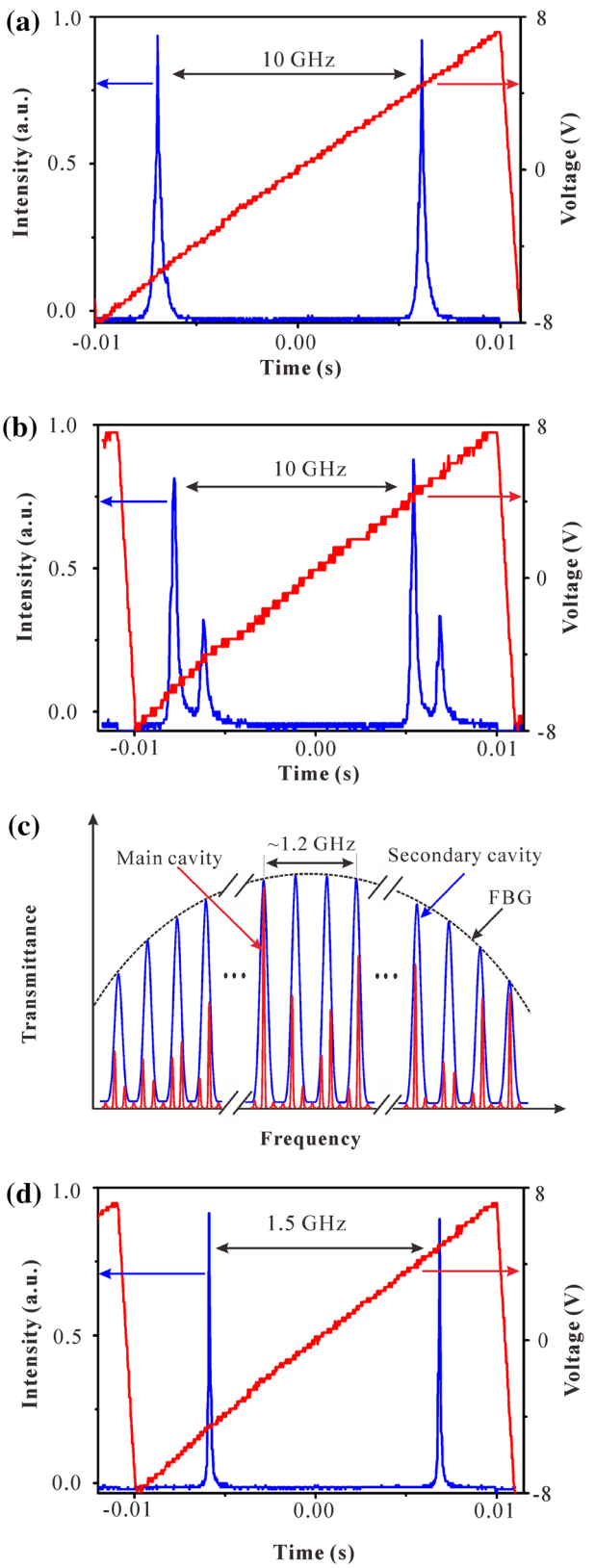


**Fig. 2** **a, b** Longitudinal mode oscillations measured by 10 GHz scanning interferometer in the condition of the SLM state when the F-P type secondary cavity is inserted only, with **b** showing the mode-hopping phenomenon; **c** schematic diagram of mode selections of the F-P type secondary cavity with the FBG, where the red curve and blue curve represent main cavity modes and secondary modes, respectively. **d** SLM state measured by 1.5 GHz scanning interferometer when all cavities are optimized. The red curve in **a**, **b** and **d** represent the sweep voltage of the F-P scanning interferometer

longitudinal modes and weakened the competition between the potential oscillation longitudinal modes. This further verifies that the strong ability of PM fiber to resist external disturbances makes it possible to optimize the cavity lengths of secondary cavities in real time according to the length of the main cavity such that the Vernier effect can be accurately used to broaden the effective longitudinal mode spacing of the compound cavity and finally effectively suppress the mode-hopping of the laser.

To monitor the stability of the SLM operation of our laser after optimizing the cavity length, the output of the laser shown in Fig. 1 was beat with the high stable SLM TSFL by the photodetector, after which the beat frequency signal was automatically recorded by the frequency counter. The result is shown in Fig. 3, in which the sudden jump of the beat signal corresponds to mode-hopping. The wavelength stability of the TSFL used in the experiment was ~ ± 5 pm in 24 h (the corresponding frequency stability was approximately ± 615 MHz/days). The measurement range of the frequency counter was 350 MHz, and the gate time was set to 100 ms in the experiment corresponding to the sampling frequency of 7 data points per second.

The automatic recording results in Fig. 3 show that the SLM stable operation time of our all-PM fiber laser is indeed ~ 15–20 min (black solid curve). However, there is a frequency shift of ~ 80 MHz/h because of the influence of environmental disturbance and the frequency instability of the TSFL. The test result of the packaged laser in the PTFE and aluminum double-decked box is also shown (green solid curve). After the vibration isolation and heat insulated packaging, the stable SLM operation time of the laser increased to a maximum of 1 h, and smooth frequency fluctuation was generally seen. The frequency drift within the 1 h operation time also reduced to 60 MHz, indicating that the packaging effectively isolates the environmental noise. However, after continuously running the laser for 3 h, the frequency drift increased to 90 MHz, and several instances of mode-hopping were observed, indicating that after the thermal insulation package, the self-heating of the laser may cause a unidirectional drift of the frequency due to temperature rise, giving rise to repeated occurrences of mode-hopping. Therefore, the packaged laser must also apply precision temperature control to ensure the long-term SLM operation stability of the laser. The red solid curve in Fig. 3 depicts the recorded beat frequency when the setting temperature is 23 ℃. It can be seen that the frequency drift is less than 30 MHz in 1 h,

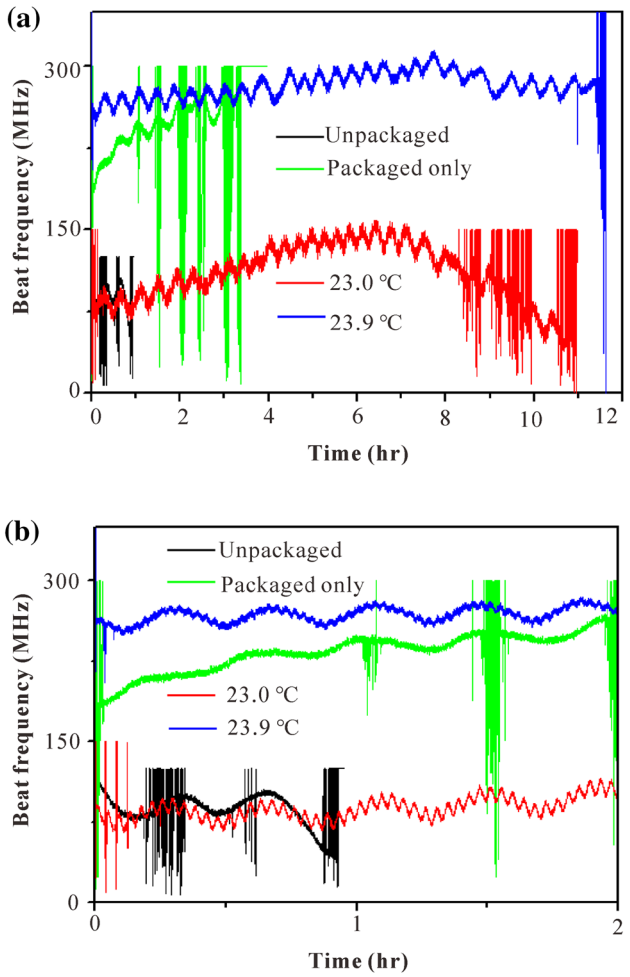


**Fig. 3** Beat signals measured automatically by the frequency counter when the laser is unpackaged (black solid curve), packaged (green solid curve), temperature-compensated at 23 ℃ (red solid curve), and temperature-compensated at 23.9 ℃ (blue solid curve) within **a** 12 h and **b** 2 h

indicating that the temperature control compensated for the self-heating of the laser, greatly reducing its frequency drift.

To more accurately use the Vernier effect, we compensated the temperature of the cavity-length-optimized compound cavity laser that was packaged with temperature control. It was found that when the heat insulation packaged laser was set at different temperatures, the SLM stable operation time was different. The blue solid curve in Fig. 3 shows the corresponding automatic recording of the beat signal when the controlled temperature was set to 23.9 °C. The stable SLM operation time of the laser was ~ 11 h, indicating that when the set temperature rose to 23.9 °C, the FSR of each cavity of the compound cavity was fine-adjusted because the length of each cavity was asynchronously increased with the increase of the temperature. The asynchronous changes in the FSRs lead to the relative movement of the transmission peaks of each cavity to the state exactly corresponding to the Vernier effect (see Fig. 2c), thereby better suppressing the mode-hopping and improving the long-term stability of the SLM operation. To the best of our knowledge, the 11-h stable SLM operation time may be the longest SLM stable operating time achieved by ring-cavity fiber lasers without feedback control. Considering that the FSR of the three cavities may differently change in a range of 90–400 Hz for the controlling precision of 0.1 °C [24], it is expected that the stable SLM operation time of our laser should still be greatly increased if the accuracy of the temperature control is improved to 0.05 °C, which is achievable with the current technology available.

Figure 4a shows the laser spectrum measured by the spectrum analyser. The central wavelength is 1560.43 nm, and the optical signal to noise ratio is an amazing 77 dB. The inset in Fig. 4a shows the laser output power as a function of the pump power; the laser threshold is 27 mW and the output power reaches 50 mW with no observed output saturation when the pump power is 580 mW, indicating that the output power can be increased further. The measured results of the laser linewidth, using a standard delayed self-heterodyne system with a 50 km single mode fiber delay line and an 80 MHz acoustic optical modulator, are shown in Fig. 4b and c, which show the results of the single scanning and the average value of 100-times scanning, respectively. The Lorentz fitting curves for the measured data are also shown. The 20 dB and 3 dB linewidths of the SLM laser are 17 kHz and 850 Hz, and 19.2 kHz and 960 Hz, respectively, according to the results shown in Fig. 4b and c. Considering that the resolution of the delayed self-heterodyne is limited by the 50 km fiber delay line, the actual 3 dB linewidth should be below 850 Hz. This is another important advantage of the inherently high $Q$ value of the ring cavity [25]. In addition, the polarization extinction ratio of the laser output is measured as high as 30 dB with a fluctuation of 0.08 dB.

## 4 Conclusions

In this study, the stability of SLM oscillation of PM-fiber-based ring compound cavity EDF lasers has been examined. Our experimental results show that because of the strong ability of PM fiber to resist environmental disturbances, the length of each secondary cavity can be optimized precisely according to the length of the main cavity in real time. Thus, the Vernier effect can be used accurately to broaden the effective longitudinal mode spacing of the compound cavity, and the mode-hopping of the laser can then be effectively suppressed. When the laser is packaged with vibration isolation and heat insulation design, the length of each cavity in the compound ring cavity fiber laser can be asynchronously fine-adjusted to further improve stability using temperature compensation control. With this compound ring cavity

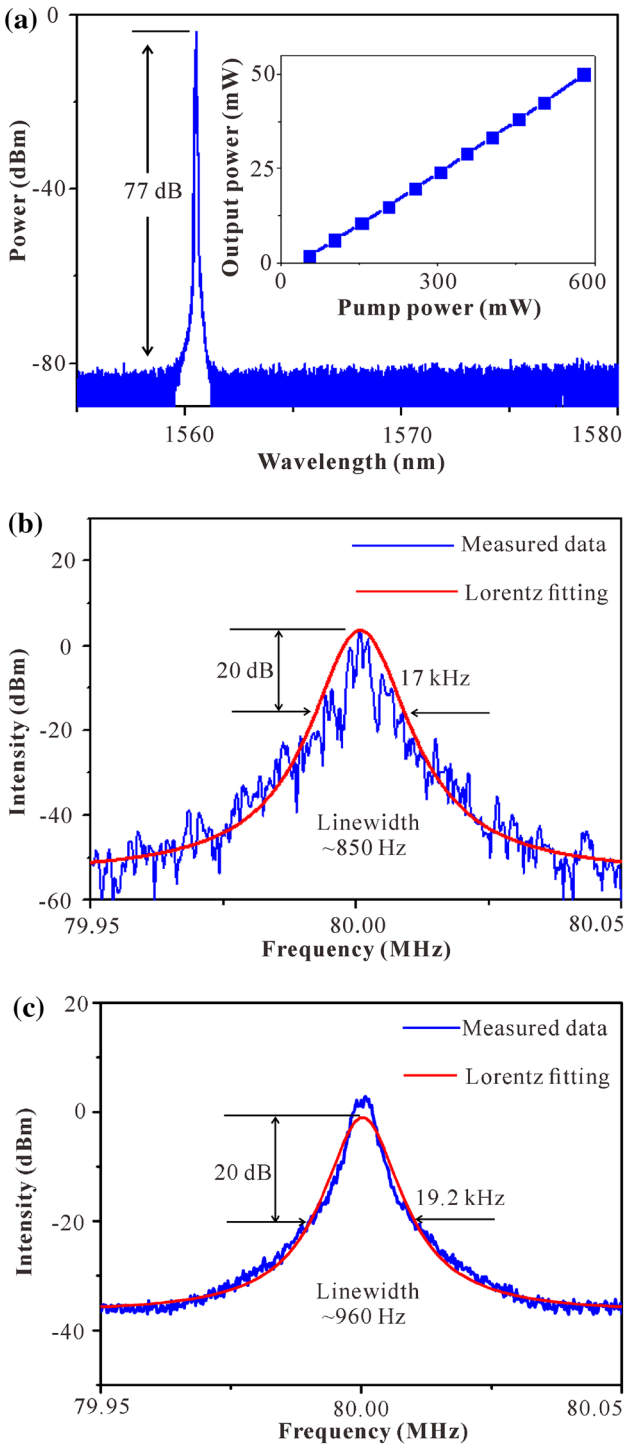


**Fig. 4** **a** Measured laser spectrum. The inset is the laser output power as a function of pump power; **b, c** measured self-heterodyne RF beating spectrum for the SLM fiber laser with 50 kmdelay fiber in the condition of: **b** the single measurement value, and **c** the average value of 100-times measurements

scheme using PM fibers, we have developed an EDF laser without mode-hopping which demonstrates an SLM operation time of ~ 11 h; meanwhile, the 3 dB linewidth of the laser output is below 850 Hz. To the best of our knowledge, this is the longest stable SLM operation time achieved without any feedback control in the ring cavity fiber laser thus far. Therefore, it is concluded that a compound ring cavity fiber laser with long-term SLM operation can be constructed using PM fibers.

**Acknowledgements** This work was supported in part by the Strategic Priority Research Program of the Chinese Academy of Sciences (XDB21010300), in part by the National key Research and Development Program of China (Grant No. 2017YFB0405100, 2017YFB0405200), in part by the National Natural Science Foundation of China (NSFC) (61805258, 61377044), and in part by the Open Research Fund of State Key Laboratory of Pulsed Power Laser Technology (SKL2017KF03).

## References

1. K. Numata, A.W. Yu, J.B. Camp, M.A. Krainak, in *Proceedings of SPIE, solid state lasers Xxvii: technology and devices*, pp. 105111D-1–105111D-7 (2018)
2. F. Theron, O. Carraz, G. Renon, N. Zahzam, Y. Bidel, M. Cadoret, A. Bresson, Appl. Phys. B. **118**, 1–5 (2015)
3. L. Duan, H. Zhang, W. Shi, X. Yang, Y. Lu, J. Yao, Sensors **18**, 3245 (2018)
4. H. Wan, J. Wang, Z. Zhang, Y. Cai, B. Sun, L. Zhang, Opt. Express **25**, 11444–11451 (2017)
5. J. Wang, H. Wanc, H. Cao, Y. Cai, B. Sun, Z. Zhang, L. Zhang, IEEE Photon. Technol. Lett. **30**, 765–768 (2018)
6. J. Zhang, Y. Chao-Yu, G.W. Schinn, W.R.L. Clements, J.W.Y. Lit, J. Lightw. Technol. **14**, 104–109 (1996)
7. C. Li, S. Xu, X. Huang, Y. Xiao, Z. Feng, C. Yang, K. Zhou, W. Lin, J. Gan, Z. Yang, Opt. Lett. **40**, 1964–1967 (2015)
8. X. Huang, Q. Zhao, W. Lin, C. Li, C. Yang, S. Mo, Z. Feng, H. Deng, Z. Yang, S. Xu, Opt. Express **24**, 18907–18916 (2016)
9. L. Dong, W.H. Loh, J.E. Caplen, J.D. Minelly, K. Hsu, L. Reekie, Opt. Lett. **22**, 694–696 (1997)
10. S. Xu, Z. Yang, W. Zhang, X. Wei, Q. Qian, D. Chen, Q. Zhang, S. Shen, M. Peng, J. Qiu, Opt. Lett. **36**, 3708–3710 (2011)
11. K. Iwatsuki, H. Okamura, M. Saruwatari, Electron. Lett. **26**, 2033–2035 (1990)
12. B. Lu, J. Kang, X. Qi, X. Feng, L. Hou, M. Jiang, H. Chen, Y. Wang, K. Wang, J. Bai, IEEE Photon. J. **9**, 1–8 (2017)
13. A. Yariv, K. Vahala, IEEE J. Quantum Electron. **19**, 889–890 (2003)
14. Q. Mao, Z. Zhu, Q. Sun, W. Liu, J.W.Y. Lit, Opt. Commun. **281**, 3153–3158 (2008)
15. Q. Mao, J.W.Y. Lit, IEEE Photon. Technol. Lett. **14**, 612–614 (2002)
16. F. Yin, S. Yang, H. Chen, M. Chen, S. Xie, IEEE Photon. Technol. Lett. **23**, 1600–1658 (2011)
17. S. Feng, Q. Mao, Y. Tian, Y. Ma, W. Li, L. Wei, IEEE Photon. Technol. Lett. **25**, 323–326 (2013)
18. T. Feng, D. Ding, F. Yan, Z. Zhao, H. Su, X. Yao, Opt. Express **24**, 19760–19768 (2016)
19. Z. Dai, X. Zhang, in *2010 Symposium on photonics and optoelectronics*. https://doi.org/10.1109/SOPO.2010.5504159 (2010)
20. Y. Chen, J.T. Kringlebotn, W.H. Loch, R.I. Laming, D.N. Payne, Opt. Lett. **20**, 875–877 (1995)
21. K. Kasai, M. Yoshida, M. Nakazawa, Opt. Express **24**, 2737–2748 (2016)

22. M. Lezius, T. Wilken, C. Deutsch, M. Giunta, O. Mandel, A. Thaller, V. Schkolnik, M. Schiemangk, A. Dinkelaker, A. Kohfeldt, A. Wicht, M. Krutzik, A. Peters, O. Hellmig, H. Duncker, K. Sengstock, P. Windpassinger, K. Lampmann, T. Hulsing, T.W. Hansch, R. Holzwarth, Optica. **3**, 1381–1387 (2016)
23. Y.H. Ja, Appl. Opt. **29**, 3517–3523 (1990)
24. H. Inaba, Y. Akimoto, K. Tamura, E. Yoshida, T. Komukai, M. Nakazawa, Electron. Commun. Jpn. Pt **2**(82), 21–29 (1999)
25. R. Poozesh, K. Madanioour, P. Parvin, J. Lightw. Technol. **36**, 4880–4886 (2018)